Shear Strength of Earth Materials in a Weathering Profile Over Granite

John Kuna Raj[1]
[1]*No.83, Jalan Burhanuddin Helmi 2, Taman Tun Dr. Ismail, Kuala Lumpur, Malaysia*
E-mail: jkr.ttdi.tmc@gmail.com

ABSTRACT: The weathering profile can be separated into an upper, 11.8 m thick pedological soil (zone I) comprising gravelly clayey sands and a lower, 31.9 m thick saprock (zone II) of silty gravelly sands that distinctly preserve the minerals, textures and structures of the original granite. Consolidated drained triaxial tests on five sets of undisturbed samples from sub-zones IC_2 (set A), IIB (set B), IIC (set C) and IID (sets D and E) yield effective cohesions (c') of 34.4 kPa, 22.7 kPa, 24.7 kPa, 27.2 kPa, and 14.5 kPa, and friction angles (ϕ') of 30.7°, 33.5°, 31.5°, 32.5°, and 34.4°, respectively. Regression analyses show the effective cohesion of samples from sub-zones IIC and IID to decrease with increasing moisture contents retained at 33 kPa, and 1,500 kPa, suction pressures; features indicating the decreasing influence of capillary and sorptive forces, respectively.

KEYWORDS: Consolidated drained triaxial tests, Effective cohesion and friction angle, Matric suction.

1. INTRODUCTION

Deep weathering profiles (several tens of meters thick) are found in Peninsular Malaysia as a result of favorable tectonic and environmental factors that have facilitated pervasive chemical weathering during a larger part of the Cenozoic era (Raj, 2009). The profiles are developed over a variety of bedrock and characterized by the indistinct to distinct preservation of the minerals, textures and structures of the original bedrock material and mass. As the earth materials of these profiles are able to be removed by commonly accepted excavating methods, they are known as residual soils in geotechnical literature in the Peninsula (USBR, 1974; JKR, 2007). The soils are also classified as unsaturated soils for they are located above the unconfined groundwater tables that are only found at the base of weathering profiles in the hilly to mountainous terrain of the Peninsula (Faisal et al., 2005; Bujang et al., 2005a, 2005b; Raj, 2009).

Residual soils are said to be of a very heterogeneous nature which makes the sampling and testing of representative parameters difficult, whilst their usually high permeability makes them susceptible to rapid changes in material properties when subjected to changes of external hydraulic condition (Tan and Gue, 2001). The shear strength parameters of the residual soils of tropical areas are, furthermore, considered to be generally higher than those of sedimentary soils (Wesley, 2009). It has thus been said that it is rare for the undrained strength of 'residual soils' to be less than about 75 kPa, whilst their effective friction angles are generally above 30° with significant values of effective cohesion (Wesley, 2009).

In a review of residual soils over granite in Peninsular Malaysia, it was concluded that "the degree of weathering process and clay content" have a significant influence on their engineering properties; the properties being similar at the same subsurface level, but varying with depth (Salih, 2012). The review also noted that the effective cohesion of these soils ranges from 7 to 77 kPa, whilst the effective friction angle was between 17° and 40°. The review finally pointed out that there is very limited published data on the determination of shear strength parameters from consolidated drained triaxial tests.

Consolidated drained triaxial tests on remolded samples of saprolite (sub-zone IC) from a residual soil over granite yielded an effective cohesion of 10 kPa, and friction angle of 28.1° (Mohd Raihan et al., 1998), whilst similar tests on another saprolite yielded effective cohesions of 8 to 9 kPa, and friction angles of 28° to 30° (Salih and Kassim, 2012). Consolidated drained triaxial tests on a clayey gravel (from saprolite in a residual soil over granite), remolded at 100 and 200 kPa, yielded effective cohesions of 8.13 and 9.04 kPa, and friction angles of 28.17° and 29.79°, respectively (Salih and Ismael, 2019). Similar tests on silty gravel (from the same saprolite), remolded at 100 and 200 kPa, furthermore, yielded effective cohesions of 1.12 and 1.42 kPa, and friction angles of 31.02° and 32.57°, respectively (Salih and Ismael, 2019).

In the course of a study on the characterization of weathering profiles in Peninsular Malaysia was investigated the profile over a coarse grained, biotite-muscovite granite at Km 16 of the Kuala Lumpur - Rawang trunk road (Route 1) (Raj, 1983). The characterization of this profile based on field mapping and differentiation of weathering zones and sub-zones followed by laboratory determination of their physical and soil index properties has been earlier discussed (Raj, submitted). The soil-moisture retention characteristics of saprock samples (from sub-zones IIC and IID) from this weathering profile have also been earlier discussed (Raj, 2021). This paper has discussed the determination of the drained shear strength parameters of earth materials at the weathering profile.

2. METHODOLOGY

The weathering profile was exposed during excavation work for widening of the Kuala Lumpur - Ipoh trunk road (Federal Route 1) close to milestone 10 (Km 16) (Figure 1). Field mapping was first carried out to differentiate weathering zones, i.e. zones of earth materials with similar morphological features as color, relict bedrock minerals, textures and structures, and litho-relicts (core stones and core boulders). Constant volume samples were then collected with brass rings at various depths to determine the physical and soil index properties of the earth materials present (Raj, submitted).

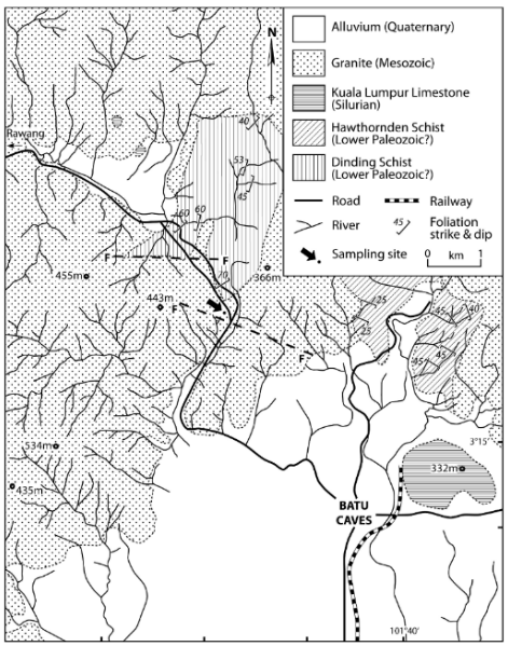

Figure 1 Geology map of Batu Caves area, Kuala Lumpur

Five sets of three samples apiece were collected for consolidated drained triaxial tests at five different depths within the weathering profile (Figure 2). The samples were collected with seamless, stainless steel tubes of 21.6 cm length and 4.06 cm internal diameter following the procedure described in the Earth Manual (USBR, 1974) for obtaining cylindrical samples by hand methods from accessible excavations. The tubes had a constant wall thickness of 0.2 cm except towards one end where the wall tapered to form a cutting edge. The tubes thus had an area ratio of 10% and an inside clearance ratio of less than 1%; ratios that allowed the collected samples to be considered as undisturbed samples (Sabatani et al., 2002). Prior to sampling, the tubes were externally greased to facilitate entry into the soil, whilst materials on the slope were removed to a depth of some 0.5 m to minimize surface effects. Each of the tubes was driven into the ground by gently hammering on a block of wood placed on its top, immediately enclosing earth materials being removed from time to time to minimize sample disturbance as per the procedure described in the Earth Manual (USBR, 1974). The tubes were then extracted from the ground by digging out the underlying soil. The ends of the sample were trimmed and sealed with solidified wax to prevent moisture loss before being taken to the laboratory.

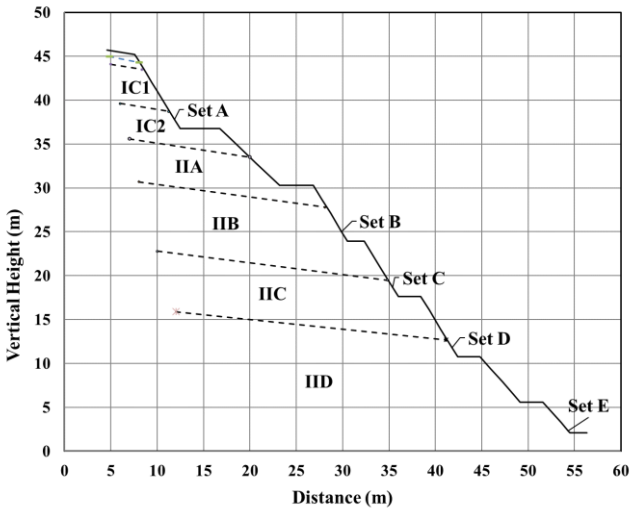

Figure 2 Sample locations and weathering sub-zones

In the laboratory, a mechanical core extruder was used to retrieve the individual samples which were trimmed to lengths of 8.9 cm and then weighed. The samples were capped at their top and bottom ends with perspex and porous discs, respectively, and then enclosed in a close fitting rubber membrane. The samples were sealed with O-rings placed around the top and bottom discs and then mounted on the pedestal of the triaxial cell. The enclosing perspex cylinder was screwed onto the base, filled with distilled water and placed under a specified pressure according to standard procedure (Bishop and Henkel, 1957). The three samples of each set were allowed to consolidate for 24 hours under cell pressures of 138 kPa, 207 kPa and 276 kPa; a 10 ml burette attached to the open drainage valve to allow recognition of any volume change. At the end of consolidation, the samples were compressed at a constant rate of 0.152 mm/min (0.006 in/min); load gauge readings on the proving ring being recorded at specified compression gauge readings. Compression was usually stopped when an axial strain of 20% was reached; the cell pressure was then reduced and water removed to describe the sample after test.

Three individual samples from each set were compressed under different cell pressures as multi-stage testing of single samples is said to produce misleading results (Tan and Gue, 2001). The deviator stress ($\sigma_1 - \sigma_3$) versus axial strain for each of the individual tests was plotted and a Mohr circle was then drawn to represent the state-of-stress at the peak value. The values of $pf = [(\sigma_1 + \sigma_3)/2]$ and $qf = [(\sigma_1 - \sigma_3)/2]$ corresponding to the peaks of the stress-strain curves of the individual specimens from each sample set were then plotted. The line drawn through the points is known as the K_f line; its gradient (ά) and intercept (a) are used to calculate the shear strength parameters of effective cohesion (c') and effective angle of friction (φ') (Lambe and Whitman, 1973).

It is to be noted that saturation of samples prior to consolidation (with the use of back-pressure) was not carried out in view of their high degree of saturation and the restricted time available for the use of the laboratory equipment. The high back pressures required for saturation are also said to increase the saturation level which then causes a reduction in effective cohesion (Salih, 2012). The effective friction angles are also not affected by soil saturation (Salih, 2012), whilst the measured values of effective cohesion are very small (Brand, 1982). It is also to be noted that the proving rings and other accessory equipment employed in the triaxial tests were calibrated in Imperial (or British) System units. Correlation factors were thus applied to the original measurements in order to convert them to SI (System International) units.

The sampling procedure adopted for the study was based on the fact that initial ground investigations classified the exposed earth materials as “cohesive soils” due to their relatively large silt and clay contents as well as high moisture contents (GEO, 2002). The use of small diameter specimens for triaxial tests was thus considered to be perfectly satisfactory; the common specimen diameter for triaxial tests of residual soils at the time of study being 37 mm (Raj, 1983; Brand and Phillipson, 1985). Larger diameter specimens will definitely reduce disturbances due to extrusion and trimming of small diameter samples (Brand and Phillipson, 1985), though sampling disturbance in residual soils has not received the attention it merits with most papers not even mentioning the subject (Sandroni, 1985). The need to minimize damage to the slope faces and more importantly the need to retain the *in situ* texture of the weathered granitic bedrock were also reasons for the use of small diameter specimens. The importance of retaining the *in situ* granitic texture has been emphasized by several workers as Mori (1985), who states that mechanical disturbance during sampling can lead to a drastic reduction in the inherent cohesive resistance of residual soils.

3. GEOLOGICAL SETTING WEATHERING PROFILE

The slope cut, at an elevation of 120 m above sea-level, is located in a fluvially dissected hilly terrain of moderate to steep ground slopes with narrow to broad, flat-bottomed valleys, some 3.5 km to the northwest of Batu Caves in Kuala Lumpur (Figure 1). Granitic and meta-sedimentary rocks are found in the general area; the meta-sediments mapped as the Dinding Schist, Hawthornden Schist, and Kuala Lumpur Limestone (Gobbett, 1965). The granites are part of the Kuala Lumpur Pluton which is a large body of irregular shape comprising two lobes located on the western side of the Main Range of Peninsular Malaysia (Cobbing et al., 1992).

Core stones and core boulders at the slope cut and nearby outcrops show the bedrock to be a coarse grained, biotite-muscovite granite that has been sheared and strongly fractured as it is located within the Kuala Lumpur Fault Zone. This Fault Zone is about 15 km wide and extends in a general southeast-northwest direction over some 100 km (Ng, 1992). The granite is characterized by mega-crysts of coarse rounded quartz and feldspars set in a groundmass of dark grey, medium to coarse grained, equigranular mosaic of quartz and feldspars, and fine biotite and muscovite flakes (Ng *et al*., 2013). Minor late phase differentiates such as microgranite, aplite and pegmatites are sometimes seen as dykes and small lenticular bodies (Yusari, 1993).

In thin-sections, the granite is holocrystalline with hypidiomorphic to allotriomorphic grains; the primary minerals being quartz, alkali feldspar, plagioclase, muscovite and biotite (Yusari, 1993). The accessory minerals include tourmaline, apatite and opaques, whilst chlorite and epidote are seen as secondary minerals. Quartz occurs as anhedral to subhedral crystals, both as phenocrysts and in the groundmass, and often shows a wavy extinction. Inclusions present include zircon, apatite and muscovite. The alkali feldspars include orthoclase and microcline and are found as euhedral to subhedral

crystals, both as phenocrysts and in the groundmass. Plagioclase feldspars generally occur as euhedral to subhedral, tabular crystals that exhibit lamellar albite twins. Extensive sericitization has occurred in the plagioclases as well as in some of the alkali feldspars (Yusari, 1993).

Both primary and secondary muscovite is present; the primary variety occurs as an individual, anhedral to subhedral grains, or as aggregates, whilst the secondary variety occurs as fine grains in feldspars due to sericitization. Biotite occurs as anhedral to euhedral individual flakes or as aggregates; some of them having been chloritized. Inclusions of zircon occur as euhedral to subhedral grains in the biotite and feldspars, whilst apatite is sometimes seen in quartz, feldspars and biotite (Yusari, 1993).

Seepage was seen at the foot of the slope cut during excavation works and indicated the presence of an unconfined groundwater table at the bottom of the exposed weathering profile.

4. WEATHERING ZONES AND WEATHERING GRADES

Field mapping shows vertical and lateral variations in the preservation of the minerals, textures and structures of the original granite; the variations allow differentiation of two broad zones, i.e. pedological soil (zone I) and saprock (zone II) (Table 1 and Figure 3). The zones are developed approximately parallel to the overlying ground surface and are of maximum thickness below the ridge crest but thin towards the valley sides.

Table 1 Morphological features of weathering sub-zones

Sub-zone	Vertical Depth (m)	Morphological features
IA	0.0-0.7	Yellowish brown, firm, sandy clay. Sub-angular blocky, moist. Dry, friable, porous. Some roots & burrows. Boundary irregular, diffuse.
IB	0.7-1.6	Strong brown, gravelly clayey sand. Firm, sub-angular blocky, moist. Friable dry. Some roots. Boundary irregular, diffuse.
IC1	1.6-6.4	Yellowish red to reddish yellow, stiff, gravelly clayey sand. Sub-angular blocky, moist. Friable dry. Boundary irregular, diffuse.
IC2	6.4-11.8	Yellowish red with red & yellow mottles. Stiff, gravelly clayey sand. Sub- angular blocky, moist. Distinct relict granite texture. Indistinct relict quartz veins. Boundary irregular, diffuse.
IIA	11.8-17.5	Friable, gravelly silty sands of yellow & red colors with yellow mottles. Sub-angular blocky, moist. Distinct relict bedrock textures & quartz veins. Indistinct relict joint planes. Some thin bands & wedges of yellowish red gravelly clayey sand. Boundary irregular, diffuse.
IIB	17.5-25.9	Friable, gravelly silty sands of mainly white & yellow colours with some red mottles. Distinct relict bedrock textures, quartz veins & joint planes. Indistinct relict fault planes. Some weathered core-stones. Boundary, irregular, diffuse.
IIC	25.9-32.8	Friable, gravelly silty sands of mainly white & yellow colours. Distinct relict bedrock textures, quartz veins, joint & fault planes. Many partly weathered to fresh core-boulders (<30% by area). Boundary irregular, diffuse.
IID	32.8-43.7	Friable, gravelly silty sands of mainly white & yellow colours. Distinct relict bedrock textures, quartz veins, joint & fault planes. Many, partly weathered to fresh core-boulders (>50% by area).

The pedological soil is some 11.8 m thick and can be differentiated into A, B and C soil horizons; the A and B horizons represent the solum, and the C horizon, the saprolite (Table 1). The solum is relatively thin (1.6 m) and consists of brown, friable to firm, gravelly sandy clay, whilst the saprolite is some 10.2 thick and comprises yellowish red, stiff, gravelly clayey sands with indistinct relict granite textures. The saprolite can be separated into upper (IC_1), and lower (IC_2), sub-zones characterized by the absence, or presence, of indistinct relict quartz veins, respectively (Table 1).

The saprock (zone II) is some 31.9 m thick and consists of silty sandy gravels to silty gravelly sands that distinctly preserve the minerals, textures and structures of the original granite; the degree of preservation increasing with depth. Zone II can be sub-divided into four sub-zones; the upper two sub-zones IIA and IIB consisting of white to yellow and red, friable, gravelly silty sands with distinct relict granite textures and quartz veins, but indistinct to distinct, relict joint and fault planes. The top IIA sub-zone with indistinct relict joint planes is 5.7 m thick and devoid of litho-relicts, whilst the lower IIB sub-zone with distinct relict joint planes, is 8.4 m thick and contains a few weathered core stones. In the lower sub-zones IIC and IID, small to large core boulders are prominent and separated by thin to broad, bands of white to yellow, friable, gravelly silty sands with distinct relict textures, quartz veins, fracture and fault planes. Core boulders form less than 30% by area of sub-zone IIC (6.9 m thick), but more than 50% of the lower IID sub-zone (10.9 m thick).

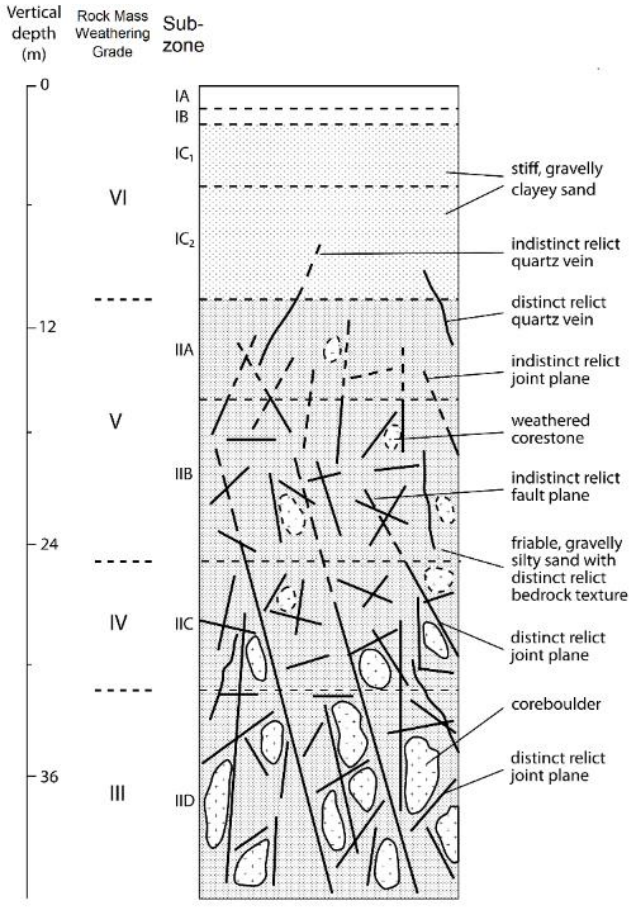

Figure 3 Morphological features at the weathering profile

Several schemes have been proposed for assigning rock mass weathering grades to weathering zones; the more widely known ones being those by IAEG (1981), GCO (1988) and GSL (1990). In terms of these published schemes, the pedological soil (zone I) would constitute rock mass weathering grade VI, whilst the bottom sub-zone IID with its' many core boulders would be classified as grade III. Sub-zone IIC would then constitute rock mass weathering grade IV, and sub-zones IIA and IIB, constitute rock mass weathering grade V (Figure 3).

The earth materials at the weathering profile are classified as residual soils in geotechnical work for their excavation has only involved scraping and ripping or "common excavation" (JKR, 2007). These residual soils are also considered to be unsaturated soils as they are located above an unconfined groundwater table (at the base of the weathering profile).

5 RESULTS

5.1 Descriptions of Sampled Earth Materials

Differences in sampling depth show the set A samples to be collected from saprolite (sub-zone IC_2), whilst the other samples (sets B, C, D and E) were collected from saprock (sub-zones IIB, IIC and IID). The samples all distinctly retain the texture (i.e. arrangement of grains) of the original granite, but show some differences in mineral composition (Table 2).

The set A samples have clay fractions of kaolinite and illite, whilst their silt fractions are entirely of sericite and the sand and gravel fractions of quartz grains that are mostly stained pink to red in color. The samples of sets B, C, D, and E also have clay fractions of kaolinite and illite, though their silt fractions are predominantly of sericite with sometimes larger muscovite flakes. The sand and gravel fractions of the saprock samples furthermore consist predominantly of vitreous quartz grains with a few white (kaolinized) and cloudy (fresh) feldspar grains (Table 2).

Table 2 Descriptions of sampled earth materials

Set (Samples)	Vertical Depth	Sub-zone	Description
Set A (1, 2 & 3)	7.39 m	IC2 (Saprolite)	Yellowish red, stiff, gravelly clayey sand. Distinct relict granite texture. Completely weathered granite. Coarse fraction: quartz grains, mostly stained pink to red & sericite flakes. Clay fraction: kaolinite & illite.
Set B (4, 5 & 6)	20.20 m	IIB (Saprock)	Yellowish white, friable, silty gravelly sand. Distinct relict granite texture. Very highly weathered granite. Coarse fraction: vitreous quartz grains, sericite & muscovite flakes & a few white (kaolinized) feldspar grains. Clay fraction: kaolinite & illite.
Set C (7, 8 & 9)	26.53 m	IIC (Saprock)	Whitish yellow, friable, silty sandy gravel. Distinct relict granite texture. Highly weathered granite. Coarse fraction: vitreous quartz grains, sericite & muscovite flakes & some white (kaolinized) feldspar grains. Clay fraction: kaolinite & illite.
Set D (10, 11 & 12)	33.40 m	IID (Saprock)	Whitish yellow, friable, gravelly sandy silt. Distinct relict granite texture. Moderately weathered granite. Coarse fraction: vitreous quartz grains, sericite & muscovite flakes & some white (kaolinized) & a few cloudy (fresh) feldspar grains. Clay fraction: kaolinite & illite.
Set E (13, 14 & 15)	42.86 m	IID (Saprock)	Whitish yellow, friable, gravelly sandy silt. Distinct relict granite texture. Moderately weathered granite. Coarse fraction: vitreous quartz grains, sericite & muscovite flakes & several white (kaolinized) and a few cloudy (fresh) feldspar grains. Clay fraction: kaolinite & illite.

5.2 Physical Properties of Sampled Earth Materials

Physical properties of samples from the different sets show minor variations; the dry unit weight ranging from 14.71 to 16.68 kN/m^3, and the dry density from 1,500 to 1,700 kg/m^3 (Table 3). The specific gravity of soil particles is of limited variation, ranging from 2.60 to 2.65, though this is to be expected in view of the similarity of the primary and secondary minerals (Table 2). Porosity is also of limited variation with all samples ranging between 36% and 42%. Interestingly enough, the saprolite sample (set A) has the maximum dry density and unit weight but minimum porosity (Table 3). Degrees of saturation are also variable; the samples (sets D and E) at depth having larger degrees of saturation (89%) than those higher up the profile (80% to 83%) (Table 3).

Table 3 Physical properties of sampled earth materials

Set	Sub- zone	Dry Unit Weight (kN/m^3)	Dry Density (kg/m^3)	Particle Specific Gravity	Porosity (%)	Moisture Content (%)	Degree Saturation (%)
Set A	IC2	17.64	1,799	2.65	32	14.3	80
Set B	IIB	17.41	1,776	2.63	33	15.1	83
Set C	IIC	17.79	1,814	2.65	32	14.1	81
Set D	IID	17.83	1,819	2.6	30	14.8	89
Set E	IID	15.9	1,622	2.65	39	21.3	89

5.3 Soil Index Properties of Sampled Earth Materials

Differences in sampling depth give rise to some variations in soil index properties; the gravel contents of samples from sets A and B being 20% and 15%, respectively, whilst those of sets C, D, and E are between 28% and 33% (Table 4). Sand contents are also quite variable; sets A and B with 43%, and 40%, respectively, whilst sets C, D, and E have contents between 25% and 27% (Table 4). Silt contents are very variable; sets A, B, C, D, and E with contents of 18%, 29%, 22%, 36% and 34%, respectively. Clay contents decrease with depth, from 19% in Set A through 16% and 18% in sets B and C, to 11% and 9% in sets D and E. Plastic limits are between 21.8% and 24.5%, except for samples of set E which have a plastic limit of 30.7% (Table 4).

Table 4 Soil index properties of sampled earth materials

Set	Sub-zone	Gravel (%)	Sand (%)	Silt (%)	Clay (%)	Plastic Limit (%)
Set A	IC2	20	43	18	19	23.6
Set B	IIB	15	40	29	16	24.5
Set C	IIC	33	27	22	18	21.8
Set D	IID	28	25	36	11	22.6
Set E	IID	31	26	34	9	30.7

5.4 Deviator Stress versus Axial Strain Curves

Plots of deviator stress (σ_1 - σ_3) versus axial strain for all specimens show a similar pattern with curves that initially rise steeply (to about 3% strain) and then gradually (to about 10% strain) before leveling off and generally dropping. Examples of these deviator stress versus axial strain curves are shown in Figure 4 for the samples of Set B from sub-zone IIB and in Figure 5 for the samples of set E from sub-zone IID. It is interesting to note that these stress-strain curves are very similar to those of consolidated drained tests on loose sand (and normally consolidated clay) where the curves also gradually rise until a peak value is reached and then become horizontal (Lambe and Whitman, 1973).

The specimens after testing developed barrel shapes (i.e. shortening and bulging around the waist) with the formation of diagonal shear planes. The peaks of the stress-strain curves thus represent the maximum stress that the specimens can support. Results of the consolidated drained triaxial tests in terms of the cell pressure (σ_3) and deviator stress (σ_1 - σ_3) at peak axial strain are listed in Table 5.

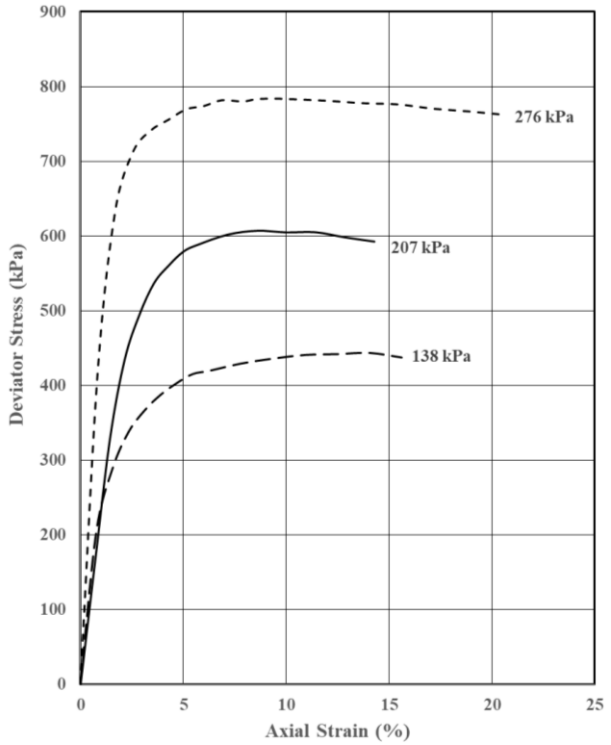

Figure 4 Deviator stress versus axial strain - Set B (sub-zone IIB)

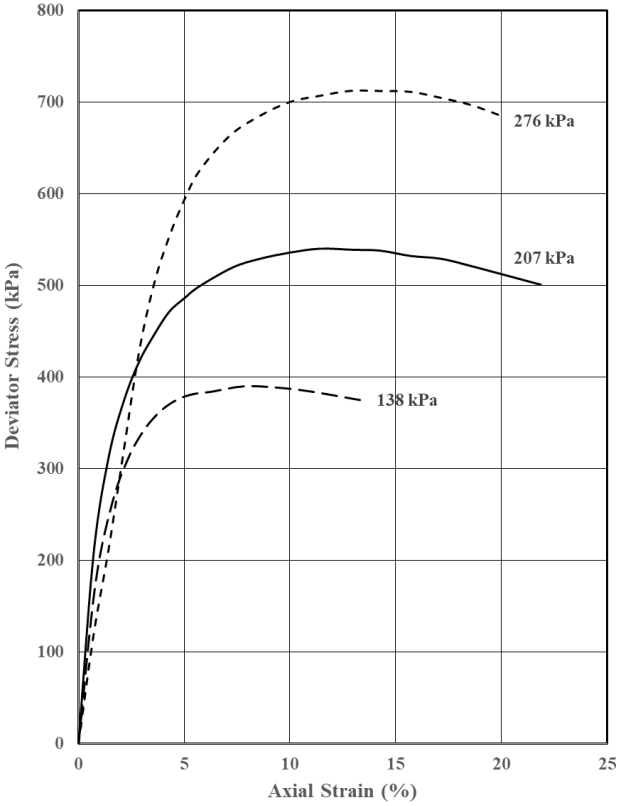

Figure 5 Deviator stress versus axial strain - Set E (sub-zone IIID)

5.5 Drained Shear Strength Parameters

Drained shear strength parameters were calculated according to the method of Lambe and Whitman (1973) where values of $pf = [(\sigma_1 + \sigma_3)/2]$ and $qf = [(\sigma_1 - \sigma_3)/2]$ corresponding to the peaks of the stress-strain curves of the three individual samples of each set were first plotted. The gradient ($\acute{\alpha}$) and intercept (a) of the K_f line drawn through the points of the three individual samples of each set was then used to calculate the shear strength parameters of effective cohesion (c') and effective angle of friction (φ') (Lambe and Whitman, 1973).

Table 5 Results of consolidated, drained triaxial tests

Set	Sample Number	Sub-zone	Peak Axial Strain (%)	Cell Pressure (kPa)	Peak Deviator Stress (kPa)
Set A	1	IC2	18.6	207	542
Set A	2	IC2	12.9	276	728
Set A	3	IC2	15.7	138	445
Set B	4	IIB	14.1	138	444
Set B	5	IIB	8.6	207	607
Set B	6	IIB	9.6	276	784
Set C	7	IIC	12.9	207	541
Set C	8	IIC	15.7	276	717
Set C	9	IIC	15	138	415
Set D	10	IID	12.5	207	605
Set D	11	IID	12.9	276	753
Set D	12	IID	17.1	138	434
Set E	13	IID	11.4	207	540
Set E	14	IID	12.9	276	712
Set E	15	IID	7.8	138	390

The calculated drained shear strength parameters show some differences with sampling depth; the saprolite (sub-zone IC) samples (Set A) having a relatively large cohesion (34.4 kPa) in comparison with those (14.5 to 27.2 kPa) of the saprock samples (Sets B, C, D and E). The saprolite samples (Set A), however, have a relatively smaller friction angle (30.7º) in comparison with those (31.5º to 33.5º) of the saprock samples (Sets B, C, D and E). When the values of $pf = [(\sigma_1 + \sigma_3)/2]$ and $qf = [(\sigma_1 - \sigma_3)/2]$ are plotted for all the saprock samples (Sets B, C, D and E), an overall effective cohesion of 19.4 kPa, and friction angle of 32.9º is determined (Table 6).

Table 6 Drained shear strength parameters of earth materials

Set	Sample Numbers	Sub-zone (Weathering Grade)	Vertical Depth (m)	Cohesion (c') (kPa)	Angle of Friction (φ')
Set A	1, 2 & 3	IC2 (VI)	7.39 m	34.4	30.7
Set B	4, 5 & 6	IIB (V)	20.20 m	22.7	33.5
Set C	7, 8 & 9	IIC (IV)	26.53 m	24.7	31.5
Set D	10, 11 & 12	IID (III)	33.40 m	27.2	32.5
Set E	13, 14 & 15	IID (III)	42.86 m	14.5	32.6
B to E	4 to 15	Saprock (III - V)		19.4	32.9

6. DISCUSSION

6.1 Comparison with Published Strength Parameters

It is to be noted that the investigated weathering profile has been differentiated into two broad weathering zones; an upper, 11.8 m thick pedological soil (zone I) of gravelly clayey sands, and a lower, 31.9 m thick saprock (zone II) of silty gravelly sands that distinctly preserve the minerals, textures and structures of the original granite. In view of differences in the physical and soil index properties of the earth materials present, it is important that comparisons with published shear strength data take into consideration the depths of samples.

In the case of saprolite (sub-zone IC) samples, the present study (set A) has determined an effective friction angle of 30.7º; a value that is in the range of 27.0º to 32.6º reported for saprolites in other weathering profiles over granite in Malaysia and Singapore (Table 7). The effective cohesion of 34.4 kPa for saprolite (set A) determined in the present study is also close to that (26 kPa) reported for saprolite in Singapore, though quite different from those of 1.1 kPa to 10.0 kPa reported for saprolites in Malaysia (Table 7). The saprolite samples investigated in Malaysia, however, are relatively coarser grained than those investigated in the present study.

Table 7 Strength parameters from consolidated drained triaxial tests

No	Soil type	Weathering Grade (Depth m)	c' (kPa)	ϕ'	Comments	Reference
1	Sandy silt (Saprolite)	VI (Depth?)	10	28.1°	Granitic soil	Mohd Raihan et al. (1998)
2	Gravelly silt (Topsoil)	VI (1.5-2.5)	8 - 9	28°-30°	Skudai, Johore	Salih & Kassim (2012)
3	Clayey gravel	VI (1.5-2.5)	8.13	28.17°	Remold 100 kPa	UTM, Johore. Salih & Ismael (2019)
			9.04	29.79°	Remold 200 kPa	
	Silty gravel (Saprolite)	VI (3.5)	1.12	31.02°	Remold 100 kPa	
			1.42	32.57°	Remold 200 kPa	
4	Residual soil	General	7 - 77	17°-40°	Literature Review	Salih (2012)
5	Sandy silt	VI (5-9)	26	27°	Multi-stage tests. Granite, Singapore	Rahardjo et al. (2004)
	Silty sand	V (10-15)	13	35°		
	Silty sand	V (15-21)	12	38°		

In the case of saprock (zone II) samples, the present study (sets B, C, D, and E) has determined effective friction angles of between 31.5° and 33.5° (with an average value of 32.9°) and effective cohesions of between 14.5 kPa and 27.2 kPa (with an average value of 19.4 kPa) (Table 6). The effective friction angles are very similar to those (31.4° to 34.4°) reported for saprock from other weathering profiles over granitic bedrock in Malaysia and Singapore (Table 7). The effective cohesions are also quite similar to those (9.5 kPa to 30.6 kPa) reported for saprock in other weathering profiles over granitic bedrock in Malaysia and Singapore (Table 7). Some differences in the values of effective cohesion and friction angle, however, are to be expected as there are differences in textures of the earth materials that have resulted from *in situ* weathering of granitic bedrock of different textures and mineral compositions. It is also to be noted that the drained shear strength parameters reported for the weathering profile over granite in Singapore were based on multi-stage consolidated drained triaxial tests; the tests causing an increase in stiffness of the samples as well as a decrease in failure strain during subsequent applications of stress (Rahardjo et al., 2003).

6.2 Factors Influencing Effective Friction Angle

The present study has determined an effective friction angle of 30.7° for saprolite samples (set A), and friction angles between 31.5° and 33.5° (with an average value of 32.9°) for saprock samples (sets B, C, D and E) (Table 6). These friction angles show little correlation with physical properties of the sampled earth materials as unit weight, density and porosity; linear regression analyses yielding variable trends with very low coefficients of determination ($R^2 < 0.160$).

In the case of the saprock samples (Sets B, C, D, and E), regression analyses yield a positive trend with a somewhat low coefficient of determination ($R^2 = 0.535$) when friction angles are plotted against sand contents; an expected trend as increased sand contents will increase inter-locking and resistance to displacement during shear (Figure 6). The regression analyses, however, yield negative trends with variable coefficients of determination when effective friction angles are plotted against gravel contents ($R^2 = 0.782$), and the total sand and gravel contents ($R^2 = 0.452$). These negative trends are somewhat unexpected, though they likely result from the large variability in gravel, sand and silt sized contents (Table 4).

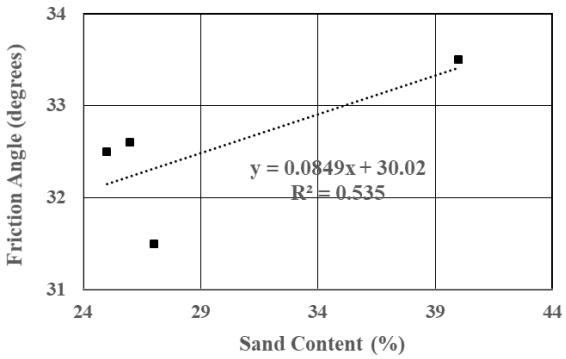

Figure 6 Effective friction angle versus sand content

6.3 Factors Influencing Effective Cohesion

The present study has determined an effective cohesion of 34.4 kPa for saprolite samples (set A) and effective cohesions between 14.5 kPa and 27.2 kPa (with an average value of 19.4 kPa) for saprock samples (sets B, C, D, and E) (Table 6). Cohesion intercepts from triaxial tests on 'residual soils' over granitic bedrock are said to reflect the existence of bonds between particles (Tan and Gue, 2001). Several causes have been proposed for these bonds and include cementation through deposition of carbonates, hydroxides and organic matter, pressure solution and re-precipitation of cementing agents as well as the growth of bonds during chemical alteration of minerals (Tan and Gue, 2001; Vaughn, 1988). Such bonds, however, are not expected in the samples of the present study for they have developed through *in situ* weathering (including leaching) of a granitic bedrock (Raj, submitted).

The effective cohesion of saprock samples (sets B, C, D, and E) furthermore show little correlation with their physical properties as unit weight, density, porosity and degree of saturation; regression analyses yielding variable trends with very low coefficients of determination ($R^2 < 0.160$). The regression analyses, however, show the effective cohesions to decrease with increasing moisture contents ($R^2 = 0.892$); a feature indicating the decreasing role of matric suction (Figure 7).

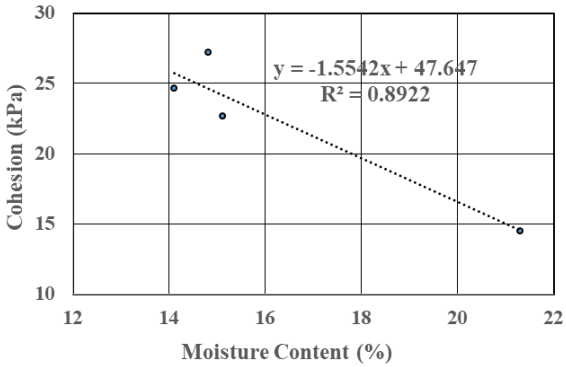

Figure 7 Effective cohesion versus moisture content

Soil-moisture retention curves of samples from sub-zones IIC and IID of the investigated weathering profile have furthermore been shown to experience decreasing gravimetric moisture contents with increasing suction pressures (Table 8) (Raj, 2021). The soil moisture retained at 33 kPa suction is of importance in Agriculture for it marks field capacity, i.e. the amount of water remaining in a soil profile after some 48 to 72 hours of free drainage following saturated conditions (Easton and Bock, 2016). The soil moisture retained at 1,500 kPa suction is also of importance in Agriculture for it marks the wilting point, i.e. the moisture content where most plants cannot exert enough force to remove water from the soil (Easton and Bock, 2016). Water

held between the field capacity and the wilting point is available for plant use, whilst capillary water held in the soil beyond the wilting point can only be removed by evaporation (Scherer et al., 1996).

Table 8 Moisture retention under different suction pressures

Sample	Vertical Depth	Gravimetric moisture content (%)				
		0 kPa	0.98 kPa	9.8 kPa	33 kPa	1500 kPa
A	26.53 m	31.9	28.6	23.3	16.9	6.8
B	31.29 m	32.1	24.9	21.5	17.8	7.4
C	41.93 m	31.6	30.3	27.3	23.5	9.5

Regression analyses show the effective cohesion of samples from sub-zones IIC and IID to decrease with increasing moisture contents retained at 33 kPa (R^2 = 0.905) suction pressure (Figure 8); a feature indicating a decrease in capillary forces (i.e. forces due to surface tension of water and its contact with solid soil particles) (Easton and Brock, 2016). The regression analyses also show the effective cohesions to decrease with increasing moisture contents retained at 1,500 kPa (R^2 = 0.848) suction pressure (Figure 8); a feature indicating a decrease in the sorptive forces that attract and bind water to the surface of soil particles (Easton and Bock, 2016; Chao and Ning, 2019). The effective cohesions of the saprock samples are therefore, considered to result from matric suction which is the sum of the capillary and sorptive forces present in partly saturated soils (Chao and Ning, 2019).

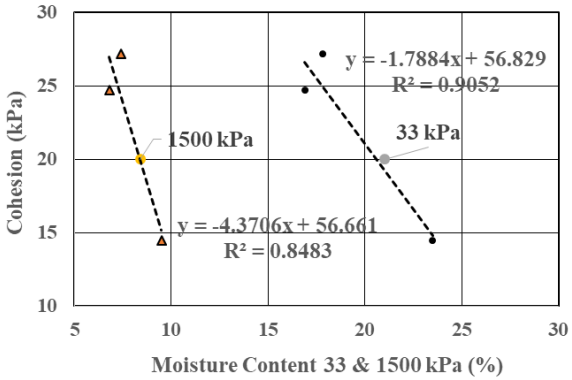

Figure 8 Effective cohesion versus moisture content retained at 33 kPa and 1,500 kPa suction pressures

Matric suction in unsaturated or partly saturated soils has furthermore, been considered to be a most important phenomenon that enhances their shear strength; some authors considering suction to be apparent cohesion (Vanapalli et al., 1996; Leong et al., 2001; Thamer et al., 2006). The occurrence of failures at slope cuts in residual soils over granitic bedrock during extended periods of rainfall can therefore, be attributed to the infiltration of rainwater and decrease in effective cohesion of the slope materials (Raj, 2000).

7. CONCLUSIONS

The weathering profile can be separated into an upper, 11.8 m thick pedological soil (zone I) comprising gravelly clayey sands and a lower, 31.9 m thick saprock (zone II) of silty gravelly sands that distinctly preserve the minerals, textures and structures of the original granite. Zone I comprises A, B and C soil horizons, whilst zone II can be differentiated into sub-zones IIA, IIB, IIC and IID, based on differences in preservation of relict structures and content of core-boulders.

Consolidated drained triaxial tests were carried out on five sets of undisturbed samples collected from sub-zones IC_2 (set A), IIB (set B), IIC (set C) and IID (sets D and E). Three samples from each set were consolidated for 24 hours under confining pressures of 138 kPa, 207 kPa and 276 kPa, and then compressed at 0.152 mm/min. Plots of Mohr-Coulomb failure envelopes yield effective cohesions (c') of 34.4 kPa, 22.7 kPa, 24.7 kPa, 27.2 kPa, and 14.5 kPa, and friction angles of 30.7°, 33.5°, 31.5°, 32.5°, and 34.4°, for sets A, B, C, D, and E, respectively.

Regression analyses show the strength parameters to have little correlation (R^2 < 0.500) with physical, and soil index, properties of the earth materials, though friction angles of saprock (zone II) samples increase with increasing sand contents (R^2 = 0.535); a feature that indicates increased inter-locking and resistance to displacement of coarse grained particles.

Regression analyses show the effective cohesion of saprock samples to decrease with increasing moisture contents (R^2 = 0.892); a feature pointing to the influence of matric suction. Regression analyses also show the effective cohesion of samples from sub-zones IIC and IID to decrease with increasing moisture contents retained at 33 kPa (R^2 = 0.905) and 1,500 kPa (R^2 = 0.848) suction pressures; features indicating the decreasing influence of capillary, and sorptive, forces, respectively. The effective cohesion of the saprock samples is thus concluded to result from matric suction which is the sum of the capillary and sorptive forces.

8. ACKNOWLEDGEMENTS

Grateful thanks are extended to the Department of Civil Engineering at the Faculty of Engineering, University of Malaya for the use of facilities at their Soil Mechanics Laboratory. Financial support for field and laboratory investigations in the preparation of this paper from an F Vote Research Grant by the University of Malaya is also gratefully acknowledged.

9. REFERENCES

Bishop, A. W. and Henkel, D. J. (1957). "The Measurement of Soil Properties in the Triaxial Test." Edward Arnold, London. 189.

Brand, E.W. (1982). "Analysis and design in Residual Soils." *Proceedings Conference on Engineering & Construction in Tropical and Residual Soils*, ASCE, Honolulu, Hawaii, 89-129.

Brand, E.W. and Phillipson, H.B. (1985). "Sampling and Testing of Residual Soils – A Review of International Practice." *Technical Committee on Sampling & Testing of Residual Soils*, International Society for Soil Mechanics & Foundation Engineering, 194.

Bujang, B.K.H., Faisal Haji Ali, and S. Hashim (2005a). "Modified shear box test apparatus for measuring shear strength of unsaturated residual soil." *American Journal of Applied Sciences*, 2, 9, 1283-1289.

Bujang, B.K.H., Faisal Haji Ali, and Affendi Abdullah (2005b). "Response of suction, moisture and temperature of unsaturated residual soil to rainfall." *Electronic Journal of Geotechnical Engineering*, 10, D, Paper 2005-0545.

Chao, Z. and Ning L. (2019). "Unitary definition of matric suction." *Journal Geotechnical & Geoenvironmental Engineering*, 145, 2. https://doi.org/10.1061/(ASCE)GT.1943-5606.0002004.

Cobbing, E.J., Pitfield, P.E.J., Darbyshire, D.P.F., and Mallick, D.I.J. (1992). "The Granites of the Southeast Asian Tin Belt." British Geological Survey Overseas Memoir 10, 369.

Easton, Z.M. and Bock, E. (2016). "Soil and soil water relationships." Virginia Cooperative Extension, Virginia Tech., Virginia State University. Publication BSE-194P. https://ext.vt.edu> agriculture>water>documents. Downloaded 17 Dec 2020.

Faisal Haji Ali, Bujang B.K. Huat and Low, T.H. (2005). "Infiltration characteristics of granitic residual soil of various weathered grades." *American Journal Environmental Sciences*, 1, 64-68.

GCO (Geotechnical Control Office) (1988). "Guide to Rock and Soil Descriptions." Geoguide 3. Geotechnical Control Office, Hong Kong, 186.

GEO (Geotechnical Engineering Office) (2002). "Guide to Site Investigation." Geoguide 2. Civil Engineering and Development Department, Government of Hong Kong Special Administrative Region. 352.

GSL (Geological Society of London) (1990). "Tropical Residual Soils." Geological Society Working Group Report, Quarterly Journal of Engineering Geology, 23, 1-102.

Gobbett, D.J. (1965). "The Lower Palaeozoic rocks of Kuala Lumpur, Malaysia." *Federation Museums Journal*, 9, 67-79.

IAEG (International Association Engineering Geology) (1981). "Rock and soil description for engineering geological mapping." *Bulletin International Association of Engineering Geology*, 24, 235-274.

JKR (Public Works Department of Malaysia) (2007). "Guidelines for Hard Material/Rock Excavation." Technical Note (Roads) 24/05. Road Division, Jabatan Kerja Raya Malaysia, 15.

Lambe, T.W. and Whitman, R.V. (1973). "Soil Mechanics." Wiley Eastern Private Ltd., New Delhi. 553.

Leong, E.C., Rahardjo, H., and Fredlund, D. D. (2001). "Application of unsaturated soil mechanics in geotechnical engineering." *Proceedings 8th East Asian Pacific Conference on Structural Engineering and Construction*, Singapore, 5-7 Dec. 2001.

Mohd Raihan Taha, Md. Kamal Hossain, Zamri Chik, and Khairul Anuar Mohd Nayan (1998). "Geotechnical behaviour of a Malaysian residual granitic soil". *Pertanika Journal of Science and Technology*, 7, 2, 151-169.

Mori, H. (1985). "Sampling and testing of granitic residual soils in Japan." In Brand, E.W. & Phillipson, H.B. (Eds), Sampling and Testing of Residual Soils – A Review of International Practice. Technical Committee on Sampling and Testing of Residual Soils, International Society for Soil Mechanics & Foundation Engineering, 99-108

Ng, T.F. (1992). "Petrography, Structure and Geotechnical Studies of the Kuala Lumpur Granite, eastern part of Kuala Lumpur, Peninsular Malaysia." M.Phil. Thesis, Institute for Advanced Studies, University of Malaya, 527.

Ng, T.F., Raj, J.K., and Azman A. Ghani (2013). "Potential alkali-reactivity of granite aggregates in the Bukit Lagong area, Selangor, Peninsular Malaysia." *Sains Malaysiana*, 42, 6, 773-781.

Rahardjo, H., Aung, K.K., Leong, E.C., and Rezaur, R.B. (2004). "Characteristics of residual soils in Singapore as formed by weathering." *Engineering Geology*, 73, 157-169.

Raj, J.K. (1983). "A Study of Residual Soils and their Cut Slope Stability in selected areas of Peninsular Malaysia." Ph.D. Thesis, Faculty of Science, University of Malaya, 462.

Raj, J.K. (2000). "Rainfall and slope failures in the granitic bedrock areas of Peninsular Malaysia." *Proceedings Annual Conference 2000*, Geological Society of Malaysia, 8 & 9 Sept. 2000, Penang, 275-282.

Raj, J.K. (2009). "Geomorphology". Chapter 2 in Hutchison, C. S. and Tan, D. N. K. (Editors), "Geology of Peninsular Malaysia." University of Malaya and Geological Society of Malaysia, Kuala Lumpur. 479. ISBN 978-983-44296-6-9.

Raj, J.K. (2021). "Soil moisture retention characteristics of saprock from a weathering profile over a biotite-muscovite granite in Peninsular Malaysia." *Newsletter, Geological Society of Malaysia*. 47, 3, 217-225.

Raj, J.K. (Submitted). "Physical characterization of the weathering profile over a coarse grained, biotite-muscovite granite in Peninsular Malaysia." *International Journal of Geo-Engineering.*

Sabatini, P.J., Bachur, R.C., Mayne, P.W., Schneider, J.A., and Zettler, T.E. (2002). "Evaluation of Soil and Rock Properties." Geotechnical Engineering Circular No.5, Report No. FHWA-IF-02-034, United States Department of Transportation. 398. https://rosap.ntl.bts.gov/view/dot/40554

Salih, A.G. (2012). "Review on granitic residual soils: Geotechnical properties." *Electronic Journal Geotechnical Engineering*, Bundle T, 17, p.2645-2658.

Salih, A.G. and Kassim, K.A. (2012). "Effective shear strength parameters of remolded residual soil." *Electronic Journal Geotechnical Engineering*, Bundle C, 17, 243-253.

Salih, A, G. and Ismael, A, M. (2019). "Influence of clay contents on drained shear strength parameters of residual soil for slope stability evaluation." *International Journal of Geotechnical Construction Materials & Environment (GEOMATE)*, 17, 59, 166-172.

Sandroni, S.S. (1985). "Sampling and testing of residual soils in Brazil." In Brand, E.W. & Phillipson, H.B. (Eds), Sampling and Testing of Residual Soils – A Review of International Practice. Technical Committee on Sampling and Testing of Residual Soils, International Society for Soil Mechanics & Foundation Engineering, 31-50.

Scherer, T. F., Franzen, D. and Cihacek, L. (2013). "Soil, Water and Plant Characteristics Important to Irrigation." AE 1675 (Revised) North Dakota State University, Extension Service. 17.

Tan, Y.C. and Gue, S.S. (2001). "The determination of shear strength in residual soils for slope stability analysis." *Proceedings Seminar Cerun Kebangsaan 2001*, Cameron Highlands, 14-15 May 2001, 1-18.

Thamer Ahmed Mohamed, Faisal Haji Ali, S. Hashim, and Bujang B.K. Huat (2006). "Relationship between shear strength and soil water characteristic curve of an unsaturated granitic residual soil." *American Journal Environmental Sciences*, 2 (4), 142-145.

USBR (United States Bureau of Reclamation) (1974). "Earth Manual." United States Government Printing Office, Washington, 810.

Vanapalli, S.K., Fredlund, D.D. and Clifton, A.W. (1996). "Model for the prediction of shear strength with respect to soil suction." *Canadian Geotechnical Journal*, 33, 3, 379-392.

Vaughan, P.R. (1988). "Characterizing the mechanical properties of in situ residual soil." Keynote Paper, *Proceedings Second International Conference on Geomechanics in Tropical Soils*, Singapore, 2, 469-487.

Wesley, L. (2009). "Behaviour and geotechnical properties of residual soils and allophone clays." *Obras y Proyectos*, 6, 5-10.

Yusari Haji Basiran (1993). "Geologi sekitaran empangan Batu - Kanching dengan penekanan kepada geokimia dan petrologi batuan granit." B.Sc. (Hons) Thesis, Department of Geology, University of Malaya. 142.